LBNL-39097
UC-404
Preprint

ERNEST ORLANDO LAWRENCE
BERKELEY NATIONAL LABORATORY

The Roles of Amorphous Grain Boundaries and the β - α Transformation in Toughening SiC

W.J. MoberlyChan, J.J. Cao, and L.C. De Jonghe
Materials Sciences Division

July 1996
Submitted to *Acta Materialia*

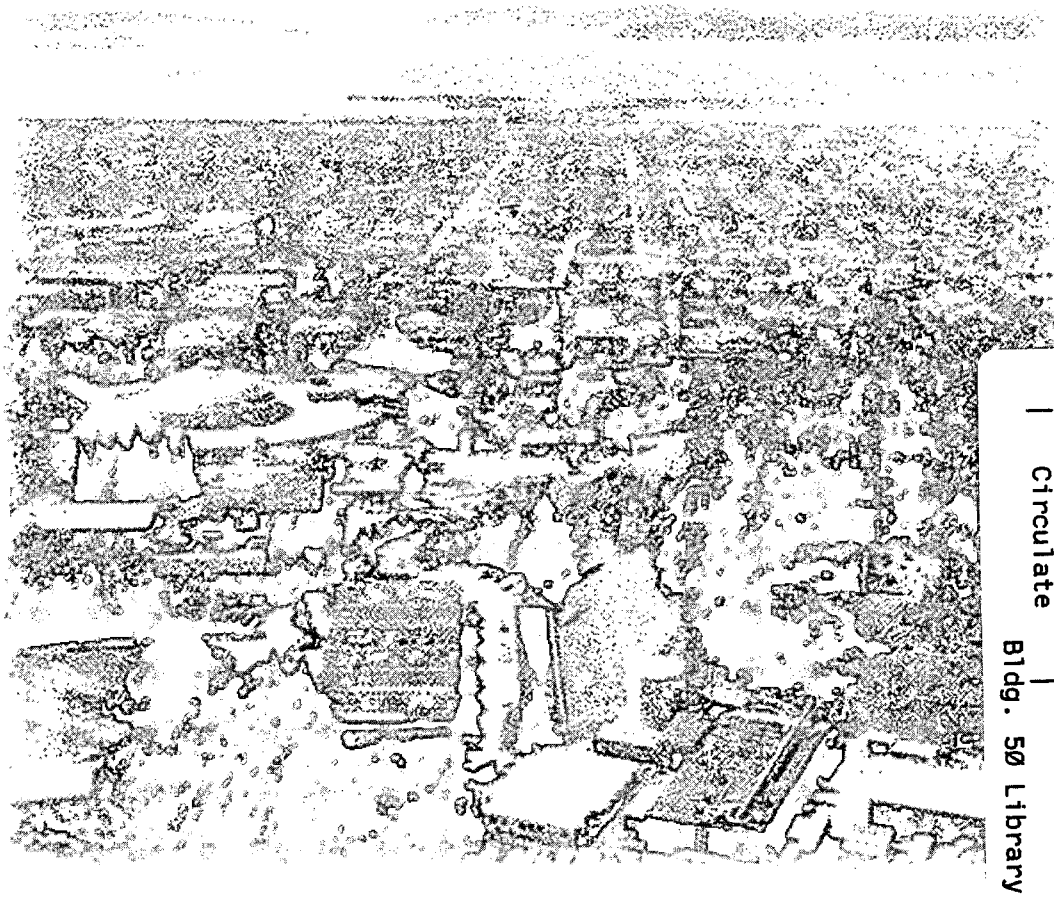

DISCLAIMER

LBNL - 39097
UC - 404

THE ROLES OF AMORPHOUS GRAIN BOUNDARIES AND THE β - α TRANSFORMATION IN TOUGHENING SiC

W. J. MoberlyChan, J. J. Cao, and L. C. De Jonghe

Department of Materials Science and Mineral Engineering,
University of California

and

MATERIALS SCIENCES DIVISION
Lawrence Berkeley National Laboratory
University of California
Berkeley, CA 94720

JULY, 1996

This work was supported by the Director, Office of Energy Research, Office of Basic Energy Sciences, Materials Sciences Division, of the U. S. Department of Energy under Contract No. DE-AC03-76SF00098.

THE ROLES OF AMORPHOUS GRAIN BOUNDARIES AND THE β - α TRANSFORMATION IN TOUGHENING SiC

W. J. MoberlyChan[1], J. J. Cao[2], and L. C. De Jonghe[2]

[1]Center for Advanced Materials, Lawrence Berkeley Laboratory, Berkeley, CA 94720

[2]Department of Materials Science and Mineral Engineering,

University of California at Berkeley, Berkeley, CA 94720

ABSTRACT

Controlled development of the ceramic microstructure has produced silicon carbide with a toughness 3 times that of a commercial SiC, Hexoloy-SA, coupled with more than 50% improvement in strength. The high toughness ceramic, ABC-SiC, was obtained by using of Al, B, and C as sintering additives; which facilitated full densification at temperatures as low as 1700°C, the formation of an amorphous phase at the grain boundaries to enhance intergranular fracture, and the promotion of an elongated microstructure to enhance crack deflection and crack bridging. Comparisons of microstructures and fracture properties have been made between the present ABC-SiC, Hexoloy-SA, and other reported SiC ceramics sintered with YAG or Al_2O_3. The Al-O chemistry of the amorphous phase in the ABC-SiC accounted for the intergranular fracture versus the transgranular fracture in Hexoloy-SA. An interlocking, plate-like grain structure developed during the β to α transformation and coupled with complete densification assured high strength and toughness.

submitted to Acta materialia
July, 1996

1. INTRODUCTION

Recent developments in the processing of SiC for improved fracture resistance have involved "*in situ* toughening" via the formation of plate-like grains during the transformation from the β-cubic to the α-hexagonal crystal structure (Suzuki [1], Mulla & Krstic [2, 3], Lee & Kim [4, 5], Padture & Lawn [6, 7], and Cao & De Jonghe [8]). The processing method utilized in this study resulted in an elongated grain structure, exhibiting a tortuous crack path associated with intergranular fracture. This provided a toughening mechanism similar to that obtained for silicon nitride [9-11]. The transformation, coupled with the development of an elongated grain structure, was induced by the use of sintering additives which promoted liquid phase sintering at temperatures 200°C to 400°C lower than the typical SiC sintering temperature of ~2100°C. Furthermore, appropriate concentrations of sintering additives and a controlled processing temperature resulted in the formation of a glassy phase at the grain boundaries, which in turn, enhanced intergranular fracture and improved toughness. Where a secondary phase coating provides a weak interface and promotes crack bridging, in both monolithic and composite material systems, it has been noted that the interfacial phase need be only slightly thicker than the interface roughness of the strengthening fiber or platelet [11-14]. Grain boundary fracture could be induced by an amorphous phase as thin as 1 nm [15, 16]. This would indicate that a minimal quantity of additives is desirable for liquid-phase-sintering: sufficient to coat grain boundaries, yet limiting the final volume fraction of secondary phases.

This study has characterized microstructural differences and commonalities between a commercial SiC (Hexoloy-SA†) and a recently developed SiC (subsequently referred to as ABC-SiC [8] indicating the sintering additives used). This ABC-SiC was toughened with plate-like grains formed during the β to α transformation. Microstructural comparisons have also been made to other SiC ceramics (referred to as Al_2O_3-SiC when Al_2O_3 is the major sintering additive [1-3], and YAG-SiC when the predominant secondary phase is amorphous and/or crystalline yttria-alumina-garnet [4-7]) toughened by similar β to α reactions. Table I lists the compositions and processing parameters reported for these "toughened" SiC ceramics. Controlling the microstructural development, both the grain shapes and the grain boundary phase(s) in the ABC-SiC has resulted in a fracture toughness more than 3 times that of Hexoloy-SA, yet with retention of high strength.

† Hexoloy SA from carborundum, Niagara Falls, NY.

TABLE I: PROCESSING PARAMETERS of TOUGHENED SiC

Name	Reference	Processing Temperature	Sintering Additives	Final Crystal Structure	Secondary Phases	Grain Length
ABC-SiC	8, 17-19	1650-1950°C	3%Al, <1%B, ~2%C	α-4H	$Al_8B_4C_7$, Al_4CO_4, Al_2O_3, B_4C	5-10 μm
YAG-SiC	4-7	1850-2000°C	5-20% YAG	α-4H, (6H if seeded)	YAG, Al_2O_3	10-25 μm
Al_2O_3-SiC	1-3	1950-2050°C	2-25% Al_2O_3	α-4H	Al_2O_3	5-15 μm

2. MATERIALS PROCESSING AND CHARACTERIZATION

Previously reported toughened SiC ceramics have typically incorporated a significant volume fraction of second phase(s), such as 5-20% Al_2O_3 [1, 2] or 10-20% YAG [5, 7]. The ABC-SiC developed here utilized ~3% Al, <1% B, and ~2% C as sintering additives. Although secondary phases also resulted from these additives, predominantly the ternary phases $Al_8B_4C_7$ and Al_4CO_4 [17-19], the transformation and observed toughening was correlated to the presence of a thin glassy phase along grain boundaries in ABC-SiC. The volume fraction of sintering additives used was a trade-off of processing parameters and properties. High aluminum content enhanced densification, lowered sintering temperature, and increased the amount of triple point phases. A smaller Al concentration lowered the fraction of detrimental secondary phases and tended to improve high temperature strength. 5 wt. % Al was necessary to provide densification of beta SiC when hot pressed for one hour at 1650°C [17, 20]; yet only 1% Al was sufficient to provide densification (>99%) at 1900°C. In addition, the size of the initial Al particles has been correlated with the resulting size of regions of the secondary phases [19, 21]. When added aluminum powders were larger than 3 micron in size, residual secondary phases were common, with only a limited amount of the additives actually incorporated as the amorphous grain boundary interlayer.

The sintering additives utilized to process the commercial Hexoloy-SA have not been extensively discussed in the literature [22, 23]. The most prominent secondary phase observed in Hexoloy-SA in this study was graphite, which was detected both within SiC grains and at large triple points. Also the porosity (>2-5%) in commercial Hexoloy-SA appeared substantially greater than that measured in the ABC-SiC.

Disks (1 to 2.5 inches in diameter) were hot pressed at 50 MPa, and at various temperatures ranging from 1650°C to 1950°C. Densification above 98% was achieved at

all temperatures by modifying the concentration of the Al sintering additive. Both pre-sintering anneals and post-sintering anneals were investigated to determine how best to control the microstructure [8]. Beams, ~3 mm square by ~30 mm long, were sliced from the hot pressed disks for 4-point bend tests to evaluate mechanical strength and fracture toughness. The tensile surfaces were polished to a <1 micron diamond finish. Although complete fracture of a bar with a controlled surface flaw has been shown to provide a more quantitative assessment of the K_{Ic} toughness [8, 24], observation of surface cracks emanating from microhardness indentations provided a good qualitative assessment of the toughness [25-27]. The measured fracture toughness of the ABC-SiC, based on the controlled surface flaw method, was 7.1 MPa$\sqrt{m}$ versus 2.2 for the Hexoloy-SA. Moreover, measurements of bend strengths yielded a value of ~650 MPa for the ABC-SiC versus ~400 MPa for the commercial Hexoloy-SA. Thus the strength, and especially the fracture toughness, of ABC-SiC compared favorably with other SiC ceramics [1-7]. Further details of processing, characterization of microstructure, and mechanical properties of these SiC ceramics have been detailed elsewhere [8, 24].

Vickers microhardness indentations were made on the polished surfaces of the ABC-SiC ceramic and the commercial Hexoloy-SA, and the lengths and configurations of cracks emanating from the corners of the indents were examined using a Scanning Electron Microscope (SEM)[i]. The crack in the Hexoloy-SA followed a relatively straight path (Figure 1a). In contrast, the cracks in the ABC-SiC (Figure 1b) exhibited deflections indicative of higher toughness. Similar comparisons of crack paths have been reported between Hexoloy-SA and the SiC "*in situ* toughened" via the incorporation of 20% YAG [7].

SEM fractography on surfaces broken in 4-point bend tests exhibited distinctive morphologies for the two SiC materials. The surface of the ABC-SiC exhibited intergranular fracture between elongated grains (Figure 2a), with bridging regions behind the crack tip (Figure 1b). The fractography of the commercial Hexoloy-SA exhibited strictly transgranular fracture, with an overall smoothness similar to brittle glasses (Figure 2b). Dark regions observed by SEM of the Hexoloy-SA (Figures 1a and 2b) were indicative of voids and occasionally secondary phases.

Bright Field Transmission Electron Microscopy (TEM)[ii] imaging defined major microstructural differences between ABC-SiC hot pressed at 1900°C and Hexoloy-SA (Figures 3 and 4, respectively). Hot pressed ABC-SiC exhibited elongated grains, with an aspect ratio greater than ten for the larger grains, which were consistent with the SEM observations of intergranular fracture around plate-like grains (Figure 2a). Much of the contrast observed within the elongated grains of ABC-SiC was from stacking faults within the α-4H microstructure. The growth of hexagonal SiC with grains elongated

---

i A Topcon ISI-DS130C was operated at 3 KeV to 20 KeV.

ii A Philips EM400 was operated at 100 KeV.

along basal planes, as well as residual stacking defects, was consistent with reported mechanisms for the beta-to-alpha transformation [28, 29]. The transformation of β-3C to α-6H has been the typical reported reaction [28, 29], however α-4H was the major transformation product observed in the present ABC-SiC. [Details of this transformation are the subject of a separate paper.] The elongated microstructure of the ABC-SiC developed during interlocking growth of plate-like grains. These interlocking grains, similar to alpha-alumina [30], would be expected to cause good creep resistance, in a more ideal manner than a microstructure of elongated, fibrous grains, such as that reported for the transformation in toughened Si_3N_4 [9-11]. The Hexoloy-SA microstructure, on the other hand, was more equiaxed, with numerous triple points exhibiting close-to-ideal 120° angles (see arrows in Figure 4). Pores were commonly observed in Hexoloy-SA, as well as secondary phase regions of graphite. The diffraction contrast within grains in Figure 4 was determined to be due to variations in thickness and bend contours. Stacking faults and microtwins, commonly observed in ABC-SiC and other SiC materials, were not present in Hexoloy-SA.

Bright Field imaging was also utilized to observe crack paths in thin TEM specimens of the ABC-SiC. The crack imaged in Figure 5 was propagated by bending a doubly-dimpled TEM sample after preparation. This particular ABC-SiC ceramic (Figure 5) had been hot pressed at 1950°C for one hour, which resulted in a larger grain size but reduced aspect ratio as compared to material hot pressed at 1900°C (Figure 3). Grain boundaries, which were not easily resolved by optical metallography nor SEM (see Figure 1b), were easily distinguished in TEM images acquired using diffraction contrast. The crack imaged in Figure 5 propagated along grain boundaries, producing a tortuous crack path similar to that observed in the SEM image of Figure 1b. The crack path did not seek out voids nor weaker secondary phases. Diffraction contrast detailed numerous stacking faults (and microtwins) within the α-4H grains of this SiC, even though it had been hot pressed at 1950°C.

High Resolution TEM[iii] was used to determine the presence of amorphous phases at the grain boundaries of both the ABC-SiC and the Hexoloy-SA (Figures 6a and 6b, respectively). For both images, the lower grain was oriented to a $<\bar{2}110>$ zone axis, with the [0001] direction normal to the grain boundary layer. As has been noted, ABC-SiC processed at the higher temperatures had been transformed to the α-4H structure with numerous stacking faults, whereas Hexoloy-SA exhibited the α-6H structure. The ABC-SiC imaged in Figure 6a had only been hot pressed at 1780°C for one hour, and therefore retained substantial β phase, both as separate β grains and as dual-phase grains comprised of α-4H and β-3C. The upper grain in Figure 6a was tilted close to a $<110>_\beta$ zone axis for high resolution imaging. On the other hand, all grain boundaries in Hexoloy-SA separated two α-6H grains. The upper grain in Figure 6b was oriented close to a $<\bar{8}\,10\,\bar{2}\,\bar{3}>_{\alpha\text{-}6H}$ zone axis for imaging.

---

iii A JEOL ARM1000 was operated at 800 Ke V, and a Topcon ISI-002B was operated at 200 KeV.

In general, no specific crystallographic relationship existed between the two zone axes orientations on either side of a grain boundary. However, the hexagonal basal plane of the lower grain (of the ABC-SiC) also represented the surface of a plate-like grain, and this grain boundary facet had to fracture intergranularly to allow for the bridging which provided the improved toughness. The grains depicted in Figures 6a and 6b were not oriented exactly along their respective zone axes, thereby sacrificing good high resolution imaging conditions. The probability was low that two randomly oriented grains had parallel, low-index zone axes, while also having a parallel grain boundary. Since the important grain boundaries (for toughness due to bridging) involved a basal plane as the long facet for one grain, this grain boundary facet was first rotated to be imaged parallel to the TEM electron beam. Subsequent tilting along the grain boundary was conducted until a compromise image within 5° of two zone axes in the adjacent grains was obtained. As long as the basal plane in the lower grain was discretely presented without tilt in the lattice image, the thickness of the amorphous grain boundary layer could be measured. The amorphous grain boundary layer observed in the ABC-SiC was always less than 2 nm and usually less than 1 nm thick. Most grain boundary layers observed in the Hexoloy-SA were also less than 2 nm thick; however, some amorphous regions were up to 5 nm thick (Figure 6b). The thicker amorphous layers in Hexoloy-SA also appeared to vary in thickness along a single grain boundary; however, this observation could have been partially inflated by imaging conditions changing due to the grain boundaries not being atomically flat and/or to subtle bending of the TEM thin foils.

The nature of TEM sample preparation of polycrystalline materials and the requirements of HR-TEM imaging precluded detection of an amorphous phase at every grain boundary. Even the grain boundary interface incorporating a basal plane had occasional steps, often 1 nm in height. On the atomic level, the grain boundaries which did not incorporate a basal plane were twisted and had numerous steps. This typically resulted in the thin amorphous boundary layer being neither parallel to the electron beam nor discrete in its projected potential throughout the thickness of the TEM specimen. Thus a (possible) thin amorphous layer often could not be observed, most probably as a result of nonideal imaging orientations. Such conditions are more pronounced for smaller grain sizes and shorter grain boundary facets; and this may account for many of the HR-TEM analyses in the literature which reported no amorphous grain boundary layer [1, 21, 23, 31-33]. Also different observed grain boundary phases or the lack of a grain boundary phase could have resulted from different sintering additives in other reports.

Techniques other than HR-TEM were utilized to corroborate the presence of this grain boundary layer. Scanning Auger Electron Spectroscopy (AES)[iv] of the fracture surfaces of ABC-SiC detected a thin alumina-containing phase on all exposed grain boundaries, which was removed with less than 1 nm ion etching (Figures 7a and 7b). The aluminum

---

[iv] A Perkin Elmer Φ-660 was operated at 3 KeV.

detected on the as fractured surface exhibited a shift in energy typical for an oxidized form of Al, such as alumina. The intensity of the O signal was diminished as compared to ideal sapphire [34], due to the thin nature of the amorphous layer and the amorphous phase being oxygen deficient. The Si present in the spectrum of the as fractured surface did not exhibit an oxidized signature, thereby indicating this signal was from the SiC grain below a thin surface layer. A trace sulfur signal was detected as fractured and after removal of <1 nm ion etching, but was removed by subsequent (>1 nm) ion etching. Weak Beam Dark Field imaging, which has been utilized in some material systems to depict amorphous films at all grain boundaries, was unsuccessful at imaging the grain boundaries in ABC-SiC. The difficulties with Dark Field imaging were due to a combination of the presence of numerous stacking defects, nonplanar grain boundaries, fine grain size, and thickness of amorphous phase often being less than 1 nm.

3. DISCUSSIONS

The higher toughness reported for the five SiC ceramics listed in the introduction (Table I), as compared to the commercial ceramic Hexoloy-SA, has been attributed to a commonality in their microstructures. All toughened SiC exhibited elongated grain structures [1-8], whereas the Hexoloy-SA displayed an equiaxed microstructure. The ABC-SiC also was comprised of a different crystal structure, α-4H, as compared to α-6H for Hexoloy-SA. The starting β-SiC powders for most of the five toughened SiC ceramics [1-8] transformed, at least partially, during processing to produce the α-4H alpha phase. One toughened SiC used seeded α-6H grains to enhance the β-α transformation [7], and XRD of the type of alpha phase was not reported for some of the SiC ceramics [2, 3, 7]. The formation of α-4H instead of α-6H has been reported as related to the presence of Al and/or Al_2O_3 as a sintering additive [1, 35], although different processing temperatures may also influence the final crystal structure. In addition, TEM and HR-TEM contrasting the commercial SiC with the ABC-SiC determined that Hexoloy-SA was essentially free of the stacking defects commonly reported for SiC. The thermal processing conditions for Hexoloy-SA have not been detailed in the literature, and it has not been published whether all starting powders were beta or alpha. However, the predominance of 120° triple points and twin-free grains suggested long times and/or high temperatures were utilized to produce the equiaxed, α-6H microstructure. In contrast, the high aspect ratio of the elongated grains of ABC-SiC was intentionally enhanced by a processing temperature lower than that utilized for other SiC ceramics.

HR-TEM determined the existence of an amorphous phase at the grain boundaries of both the ABC-SiC and the commercial Hexoloy-SA. However, the thin nature of this interfacial layer prevented a conclusive chemical analysis by traditional analytical TEM. (Energy Filtered Imaging has established an enrichment of Al and O at or near the grain boundaries of ABC-SiC [36].) Coupled with AES analysis of the intergranular fracture

surfaces, the amorphous layer in the ABC-SiC was determined to be an Al (and O)-containing glassy phase. Since the Hexoloy-SA material did not fracture along grain boundaries, and the sintering additives used to process this commercial ceramic have not been published, the chemistry of the amorphous layer in the Hexoloy-SA has not yet been ascertained. Although the exact effect of amorphous phase chemistry on intergranular fracture could not be assessed, the observed difference in fracture mode indicated chemistry of the amorphous phase was more critical than thickness.

The chemistry of an amorphous grain boundary necessary to induce intergranular fracture appeared to be more subtle than just the presence of a glassy, oxide phase. Auger electron spectroscopy of the ABC-SiC boundaries not only exhibited alumina-bonding but also a trace of sulfur. Furthermore, the sulfur impurity appeared to be preferentially segregated between the SiC and the Al-containing layer. Other analyses of glassy grain boundary phases also have observed "secondary" impurities. In SiC, sintered with Al_2O_3 additives, Suzuki [1] discussed the presence of Ca on intergranular fracture surfaces. Other work [37, 38] has also indicated the presence of Ca segregated between the glassy phase and the Si_3N_4 grain, as well as its influence on altering the thickness of the amorphous phase. Computer modeling has established the influence of S impurities to weaken grain boundaries [39]. The influence of sulfur impurities in SiC, as well as control of their location within the grain boundary, is being pursued with further experimental observations [38, 40].

The grain sizes of the five tough SiC ceramics listed in Table I varied from 2 to 25 microns in length [1-8]. The grain size of the Hexoloy-SA and the ABC-SiC were similar, ranging from 5 to 10 microns. However, the aspect ratio upwards of 10 in the ABC-SiC ceramic differed considerably from the equiaxed grains of the Hexoloy-SA. The aspect ratio, in conjunction with intergranular fracture provided high toughness in ABC-SiC. Analysis of monolithic SiC, sintered with the same Al, B, and C additives at a temperature low enough to prevent the β to α transformation, also detected an alumina-containing amorphous grain boundary [19, 21]. These weak interfaces promoted intergranular fracture; however, the more equiaxed shape of the submicron beta grains did not allow for enhanced toughening due to grain bridging. Thus, high toughness in this ceramic required an amorphous grain boundary layer, a chemistry to weaken the grain boundary, and a grain shape with a high aspect ratio. Lack of any of these three ingredients produced an inherently brittle material.

Analyses of the two reported Al_2O_3-SiC have indicated both similarities and disparities as compared to the present ABC-SiC. Since the Al in the ABC-SiC partially reacted with oxides on the surface of SiC powders, the alumina-containing glassy phase at the grain boundaries of ABC-SiC could have acted similarly to the Al-containing impurities on the intergranular fracture surfaces of Al_2O_3-SiC [1]. Although Suzuki [1] detected Al on intergranular fracture surfaces with Auger, he did not observe an amorphous phase by HR-TEM in the same material. Other reported Al_2O_3-SiC [2, 3] did not include Auger

analysis of fracture surfaces nor HR-TEM of grain boundaries. The disparity in Suzuki's AES and HR-TEM data could be attributed to the fact that the Suzuki's HR-TEM images did not depict one of the {0001} planar grain boundaries. Other research of grain boundaries in SiC typically did not resolve cross fringes to make analysis of the boundary unambiguous [1, 23, 31-33]. ABC-SiC sintered at lower temperatures also exhibited some grain boundaries without an amorphous phase being detected by HR-TEM [17, 21]. Yet, the analysis of amorphous layers <1 nm thick along nonplanar boundaries in fine-grained polycrystalline materials was recognized as subject to numerous difficulties [21]. Conflicting published reports exhibiting both the presence and lack of amorphous grain boundaries could represent respective differences between random and special orientation relationships across grain boundaries, and/or differences in processing conditions. Whenever AES of intergranular fracture surfaces has detected substantial chemical impurities along grain boundaries, it was believed that corresponding HR-TEM images were inconclusive if they did not depict an amorphous nor a crystalline intergranular phase.

The SEM analyses reported for the two YAG-SiC ceramics (sintered with >10% YAG) clearly showed a similar rough crack path around the elongated alpha SiC grains [4-7]. The crack paths suggested more the presence of grain boundary deflection rather than grain pullout. However, a TEM analysis of the grain boundaries has not been reported for either YAG-SiC ceramic [4-7]. Nor has it been determined whether the YAG is fully crystalline or amorphous. Since the volume fraction of YAG was substantial, most SiC grains were coated with a relatively thick layer of YAG, and SEM images showed that the crack path remained in the YAG. With the large amount of YAG (up to 20% by volume), these YAG-SiC ceramics could be considered as composites, with the YAG being a "weak" phase and an easy path for crack propagation. In many SEM images the YAG formed a nearly continuous network, and therefore would have provided a simple means for all crack propagation to have occurred within the YAG. Thus, when a continuous, and relatively thick, network of YAG existed, the propagation of the crack through the YAG suggested much of the strength of the composite was dependent on this weaker phase. Although the fracture toughness was improved, the room temperature strength of YAG-SiC was reduced as compared to Hexoloy-SA [7]. In contrast, the lower concentration of sintering additives in the ABC-SiC enabled a much higher fracture strength to be realized.

Since the primary utility of these toughened SiC ceramics is for high-temperature structural applications, the effects of microstructure (and residual additives) on high temperature strength must be considered. However, no high temperature mechanical testing of these YAG-SiC ceramics nor of ABC-SiC have yet been published. The decrease in strength of YAG at high temperatures [41], should correspond to a decrease in strength of SiC containing 10-20% YAG, especially for an amorphous secondary phase. YAG-SiC offered the possibility of good ductility at high temperature [7], but with a degradation in strength. The thin amorphous phase in the ABC-SiC also has been

expected to enhance creep, as has been reported for Si_3N_4 [42]. However, the amorphous phase had a minimal thickness, and residual triple point pockets were typically crystalline ternary phases [36]. Since SiC has a higher melting temperature than does Si_3N_4, an improved creep resistance would be expected as compared to Si_3N_4 at similar temperatures. Further work has been initiated to determine which microstructures would provide the best compromise of high temperature strength and room temperature toughness [43].

The improved fracture toughness of YAG-SiC was reported to be due to a corresponding increase in "short crack" formation [7]. This was speculated [7] to occur (in part) as a result of stress arising from a mismatch in coefficient of thermal expansion (CTE) between the SiC and YAG. Such CTE mismatches would be a further reason for limiting the volume fraction of a second phase. A tortuous crack path which occurred because it was connecting-up numerous, pre-existing short cracks would provide a rough fracture surface, but would also correlate to a lowering of the overall fracture strength.

In the ABC-SiC no pre-existing cracks were observed after processing. In addition, the tortuous crack paths, which were propagated during mechanical testing, did not connect pockets, greater than one micron in size, of (weaker) secondary phases. Cracks propagating along grain boundaries were further deflected by small (5-10 nm) crystalline triple points. However, "over-sintering" at temperatures above 1900°C led to small voids at triple points, which may correlate to reductions in strength and toughness [8]. Nevertheless, nanometric-scale voids at triple points would be expected to have less detrimental effects on strength than other toughening mechanisms, such as pre-existing cracks and/or 10%-20% of a weaker phase.

The deflection of the crack around elongated grains (Figure 1b) and the observations of crack bridging (Figure 2a) have provided a similar toughening mechanism as reported for the YAG-SiC ceramics. The interlocking nature of the plate-like ABC-SiC grains hindered a simple pullout mechanism as have been proposed for the fiber-like grains of Si_3N_4 [10, 11]. Furthermore, the ABC-SiC exhibited less crack branching than the YAG-SiC ceramics, especially far from the main crack surface. The presence of fewer short cracks, a lower volume fraction of secondary phases, and an interlocking grain morphology correlated to the substantially higher strength obtained for this ABC-SiC.

4. SUMMARY

Both the recently developed ABC-SiC and the commercial SiC (Hexoloy-SA) had an alpha hexagonal crystal structure and a grain size ranging from 3 to 10 microns. In addition, both materials exhibited an amorphous phase at the grain boundaries, resulting from the sintering additives used. However, the ABC-SiC started with submicron beta powder and used sintering additives (Al, B and C) which enabled liquid phase sintering at temperatures below which are typically reported for SiC. The β-to-α phase transformation could be controlled at these lower temperatures to produce an interlocking, plate-like microstructure consisting of α-4H grains rather than the equiaxed α-6H grains in Hexoloy-SA. The elongated grains (with an aspect ratio upwards of 10) in the ABC-SiC enabled cracks to deflect through the weaker amorphous phase at the grain boundaries, resulting in bridging of grains behind the propagating crack tip. This microstructure enhanced the toughness of ABC-SiC by a factor of 3 over that of the commercial Hexoloy-SA as well as providing >50% improvement in strength.

ACKNOWLEDGMENTS

This work was supported by the Director, Office of Energy Research, Office of Basic Energy Sciences, Materials Sciences Division, of the United States Department of Energy under Contract No. DE-AC03-76SF00098 with the Lawrence Berkeley Laboratory. Also the authors wish to thank R. Cannon, C. Gilbert, M. Gopal, R. Ritchie, M. Sixta, and G. Thomas for their technical assistance and discussions. The authors were grateful for use of the facilities of the National Center for Electron Microscopy, and especially for the assistance of staff members D. Ah-Tye, C. Nelson, and J. Turner.

REFERENCES

1. K. Suzuki, "Pressureless-Sintered Silicon Carbide with Addition of Aluminum Oxide," in *Silicon Carbide Ceramics V2* (edited by S. Somiya and Y. Inomata, Elsevier Applied Science, 163-182 (1991).
2. M. A. Mulla and V. D. Krstic, "Pressureless Sintering of β-SiC with Al_2O_3 Additions," *J. Matls. Sci.* **29**, 934-938 (1994).
3. M. A. Mulla and V. D. Krstic, "Mechanical Properties of β-SiC Pressureless Sintered with Al_2O_3 Additions," *Acta metall. mater.* **42** [1] 303-308 (1994).
4. D. H. Kim and C. H. Kim, "Toughening Behavior of Silicon Carbide with Additions of Yttria and Alumina," *J. Am. Ceram. Soc.* **73** [5] 1431-1434 (1990).
5. S. K. Lee and C. H. Kim, "Effects of α-SiC versus β-SiC Starting Powders on Microstructure and Fracture Toughness of SiC Sintered with Al_2O_3-Y_2O_3 Additives," *J. Am. Ceram. Soc.* **77** [6] 1655-1658 (1994).
6. N. P. Padture, "*In Situ*-Toughened Silicon Carbide," *J. Am. Ceram. Soc.* **77** [2] 519-523 (1994).
7. N. P. Padture and B. R. Lawn, "Toughness Properties of a Silicon Carbide with an *in Situ* Induced Heterogeneous Grain Structure," *J. Am. Ceram. Soc.* **77** [10] 2518-2522 (1994).
8. J. J. Cao, W. J. MoberlyChan, L. C. De Jonghe, C. J. Gilbert, and R. O. Ritchie, "*In Situ* Toughened Silicon Carbide with Al-B-C Additions," *J. Amer. Ceramic Soc.* **79** [2] 461-469 (1996).
9. F. F. Lange, "Relation between Strength, Fracture Energy and Microstructure of Hot-Pressed Si_3N_4," *J. Am. Ceram. Soc.* **56** [10] 518-522 (1973).
10. C.-W. Li, D.-J. Lee, and S.-C. Lui, "R-Curve behavior and Strength for *in situ* Reinforced Silicon Nitrides with Different Microstructures," *J. Am. Ceram. Soc.* **75** [7] 1777-1785 (1992).
11. P. F. Becher, "Microstructural Design of Toughened Ceramics," *J. Am. Ceram. Soc.* **74** [2] 256-269 (1991).
12. K. H. Kim, K. G. Sheppard, W. J. Moberly, K. Chyung, and W. C. Oliver, "Study of Fiber/Matrix Interface in SiC(Nicalon) Fiber-Reinforced Calcium Aluminosilicate Matrix Composites", Am. Ceram. Soc. 1992 Conf. Proc.
13. C. H. Hsueh, "Evaluation of Interfacial Shear Strength, Residual Clamping Stress, and Coefficient of Friction for Fiber-reinforced Ceramic Composites," *Acta metall. mater.* **38** [3] 403-409 (1990).
14. J. D. Bright, D. K. Shetty, C. W. Griffin, and S. Y. Limage, "Interfacial Bonding and Friction in Silicon Carbide (Filament)-Reinforced Ceramic- and Glass-Matrix Composites," *J. Am. Ceram. Soc.* **72** [10] 1891-1898 (1989).
15. D. R. Clarke, "On the Equilibrium Thickness of Intergranular Glass Phase in Ceramic Materials," *J. Am. Ceram. Soc.* **70** [1] 15-22 (1987).

16. H.-J. Kleebe, M. K. Cinibulk, R. M. Cannon, and M. Rühle, "Statistical Analysis of the Intergranular Film Thickness in Silicon Nitride Ceramics," *J. Am. Ceram. Soc.* **76** [8] 1969-1970 (1993).
17. T. D. Mitchell, L. C. DeJonghe, W. J. MoberlyChan, and R. Ritchie, "Silicon Carbide Platelet / Silicon Carbide Composites," *J. Am. Ceram. Soc.* **78** [1] 97-103 (1995).
18. J. J. Cao, W. J. MoberlyChan, L. C. De Jonghe, B. Dalgleish, and M. Y. Niu, "Processing and Characterization of SiC Platelet / SiC Composites," in *Advances in Ceramic-Matrix Composites II, Ceramic Transactions* **46**, 277-288 (1995).
19. W. J. MoberlyChan, J. J. Cao, M. Y. Niu, and L. C. De Jonghe, "Toughened β-SiC Composites with Alumina-Coated α-SiC Platelets," in *High Performance Composites* (edited by K. K. Chawla, P. K. Liaw, and S. G. Fishman), TMS Conf. Proc. (1994).
20. B.-W. Lin, M. Imai, T. Yano, and T. Iseki, "Hot-Pressing of β-SiC Powder with Al-B-C Additives," *J. Am. Ceram. Soc.* **69** [4] C67-C68 (1986).
21. W. J. MoberlyChan, J. J. Cao, M. Y. Niu, L. C. De Jonghe, and A. F. Schwartzman, "SiC Composites with Alumina-Coated α-SiC Platelets in β-SiC Matrix: Controlling Toughness Through Microstructure," in *Microbeam Analysis Proceedings* (edited by J. Friel) VCH Publ., NY, 49-50 (EMSA 1994).
22. S. Dutta, "Sinterability, Strength and Oxidation of Alpha Silicon Carbide Powders," *J. Matls. Sci.* **19**, 1307-1313 (1984).
23. K. Y. Chia and S. K. Lau, "High Toughness Silicon Carbide," *Ceram. Eng. Sci. Proc.* **12** [9-10] 1845-1861 (1991).
24. C. J. Gilbert, J. J. Cao, W. J. MoberlyChan, L. C. De Jonghe, and R. O. Ritchie, "Cyclic Fatigue and Resistance-Curve Behavior of an *In Situ* Toughened Silicon Carbide with Al-B-C Additions, " *Acta metall. mater.* (in press).
25. R. H. Marion, "Use of Indentation Fracture to Determine Fracture Toughness," in *Fracture Mechanics Applied to Brittle Materials* (edited by S. W. Friedman) ASTM STP 678, 103-111 (1979).
26. R. W. Hertzberg, in *Deformation and Fracture Mechanics of Engineering Materials, 3rd Ed.* J. Wiley, NY, 302-304 (1989).
27. G. R. Anstis, P. Chantikul, B. R. Lawn, D. B. Marshall, "A Critical Evaluation of Indentation Techniques for Measuring Fracture Toughness: I, Direct Crack Measurements," *J. Am. Ceram. Soc.* **64** [9] 533-538 (1981).
28. L. U. Ogbuji, T. E. Mitchell, and A. H. Heuer, "The β to α Transformation in Polycrystalline SiC: III, The Thickening of α Plates," J. *Am. Ceram. Soc.* **64** [2] 91-99 (1981).
29. P. Pirouz and J. W. Yang, "Polytypic Transformations in SiC: The Role of TEM," *Ultramicroscopy* **51**, 189-214 (1993).
30. L. C. De Jonghe, "Grain Boundaries and Ionic Conduction in Sodium Beta Alumina," *J. Matls. Sci.* **14**, 33-48 (1979).

31. S. Shinozaki, J. Hangas, K. Maeda, A. Soeta, "Enhanced Formation of 4H Polytype in Silicon Carbide Materials," in *Silicon Carbide Ceramics 87, Amer. Ceramic Soc. Transactions*, 113-121 (1987).
32. K. Nakamura and K. Maeda, "Hot-pressed SiC Ceramics," in *Silicon Carbide Ceramics V2* (edited by S. Somiya and Y. Inomata) Elsevier Applied Science, 139-162 (1991).
33. S. S. Shinozaki, J. Hangas, K. R. Carduner, M. J. Rokosz, K. Suzuki, and N. Shinohara, "Correlation Between Microstructure and Mechanical Properties in Silicon Carbide with Alumina Addition," *J. Mater. Res.* **8** [7] 1635-1643 (1993).
34. L. E. Davis, N. C. MacDonald, P. W. Palmberg, G. E. Riach, and R. E. Weber, in *Handbook of Auger Electron Spectroscopy* Physical Electronics Industries (1976).
35. S. Shinozaki, R. M. Williams, B. N. Juterbock, W. T. Donlon, J. Hangas, and C. R. Peters, "Microstructural Developments in Pressureless-Sintered β-SiC Materials with Al, B, and C Additions," *Am. Ceram. Soc. Bull.* **64** [10] 1389-1393 (1985).
36. W. J. MoberlyChan, J. J. Cao, and L. C. De Jonghe, "The Crystallography of Triple Points in Nonoxide Ceramics: Epitaxial Relationships Are a Function of Statistics and Geometry," (EMSA 1996 Proceedings, in press).
37. I. Tanaka, et al, "Calcium Concentration Dependence on the Intergranular Film Thickness in Silicon Nitride," *J. Am. Ceram. Soc.* **77** [4] 911-914 (1994).
38. H. Gu, et al, "Chemistry of Intergranular Phases in Si_3N_4 by Spatially Resolved Electron Energy-Loss Spectroscopy," (presented at ACS, Cinn., May, 1995).
39. D. J. Srolovitz, T. Hong, J. Raynolds, and G. L. Zhao, "Impurity Effects on Interfacial Adhesion: Simple Lessons From *ab initio* Calculations," *Matls. Res. Soc. Proc.* **V409**, Fall 1995 (in press).
40. R. Cannon, Personal communications.
41. K. Keller, T. Mah, and T. A. Parthasarathy, "Processing and Mechanical Properties of Polycrystalline $3Y_2O_3 \cdot 5Al_2O_3$ (Yttrium Aluminum Garnet)," *Ceram. Eng. Sci. Proc.* **11** [7-8] 1122-1133 (1990).
42. M. M. Chadwick, R. S. Jupp, and D. S. Wilkinson, "Creep Behavior of a Sintered Silicon Nitride," *J. Am. Ceram. Soc.* **76** [2] 385-396 (1993).
43. J. McNaney, R. O. Ritchie, work in progress.

FIGURES

Fig. 1a.
SEM micrograph of crack path that emanated from the corner of a Vickers microhardness indentation made on the polished surface of a commercial SiC, Hexoloy-SA. Dark features in the Hexoloy-SA were indicative of porosity in this material.

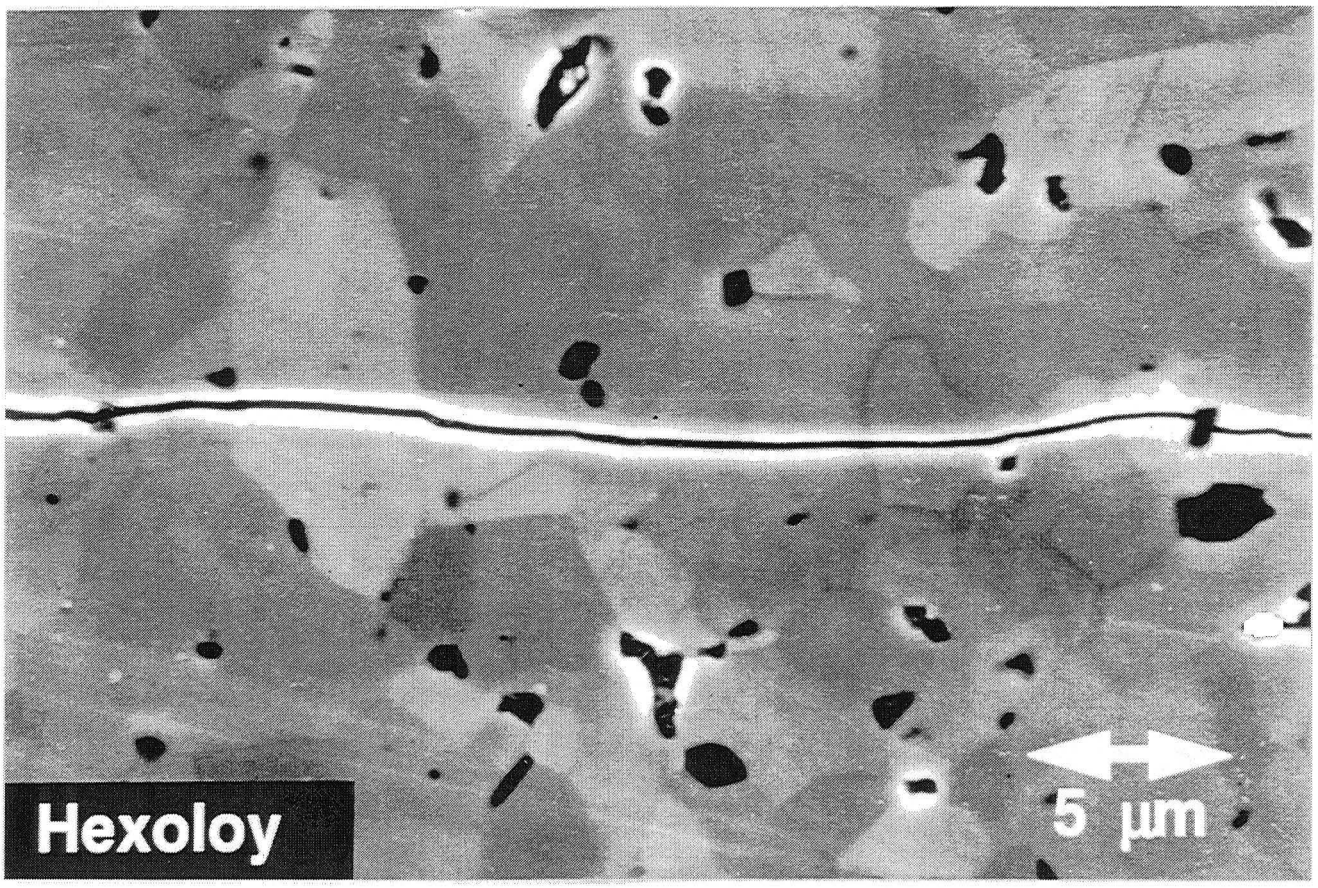

Fig. 1b.

SEM micrograph of crack path that emanated from the corner of a Vickers microhardness indentation made on the polished surface of ABC-SiC. The crack path deflected around elongated grains of ABC-SiC and did not deflect toward secondary phases, characterized as $Al_8B_4C_7$, Al_4CO_4, Al_2O_3, and B_4C.

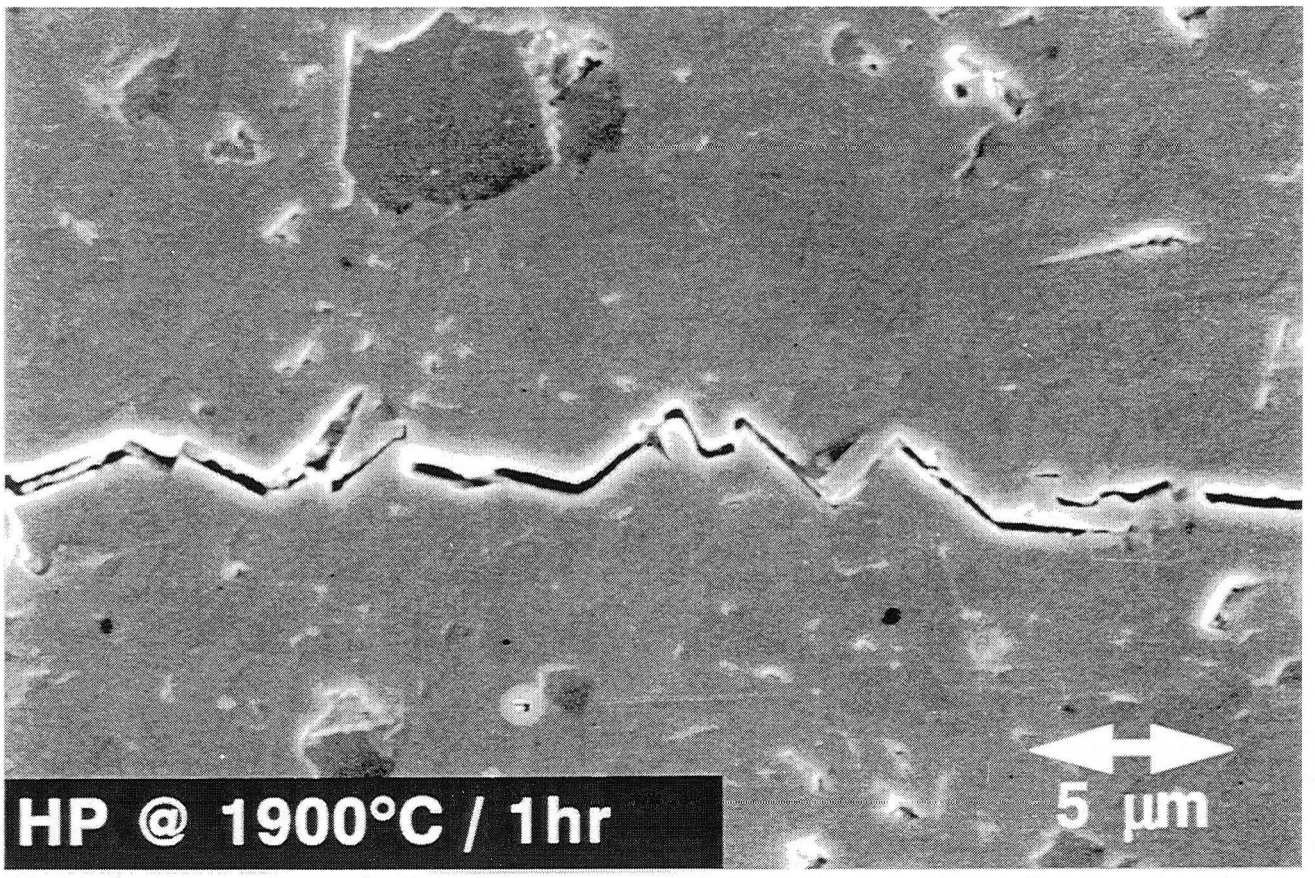

2. SEM fractographs of ABC-SiC hot pressed at 1900°C for 1 hour (2a) and of Hexoloy-SA (2b), from controlled flaw bending tests. The tortuous surface morphology in ABC-SiC resulted from intergranular fracture and bridging of elongated, plate-like α-4H grains. The surface morphology of the Hexoloy-SA indicated transgranular fracture of the α-6H grains.

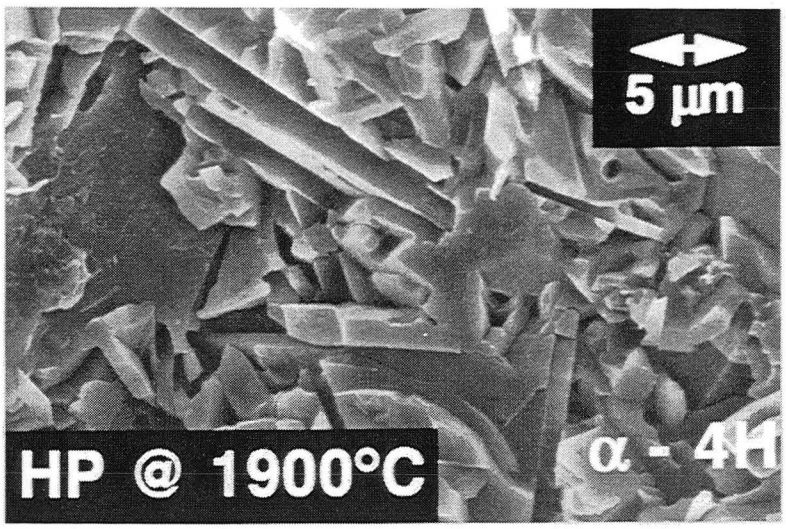

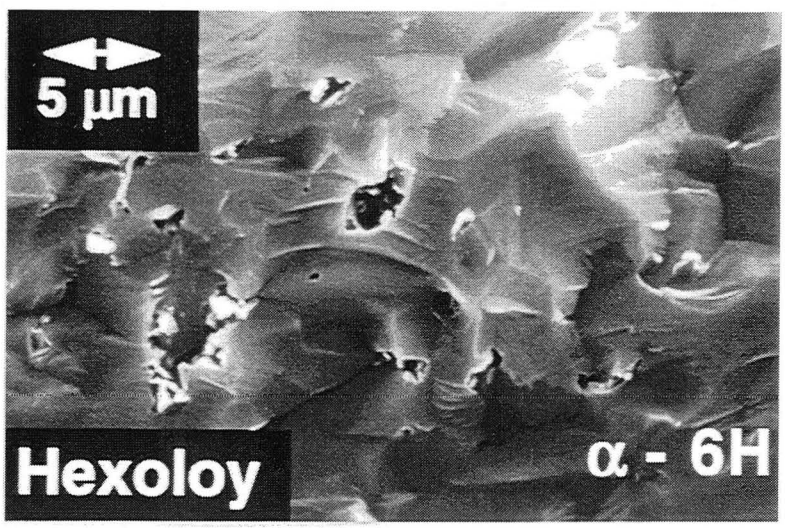

3. Bright field TEM image of the microstructure of ABC-SiC hot pressed at 1900°C for 1 hour. Elongated, plate-like grains, with an interlocking microstructure developed during the β to α phase transformation. Streaks within grains were determined to be stacking faults and microtwins in the α-4H structure.

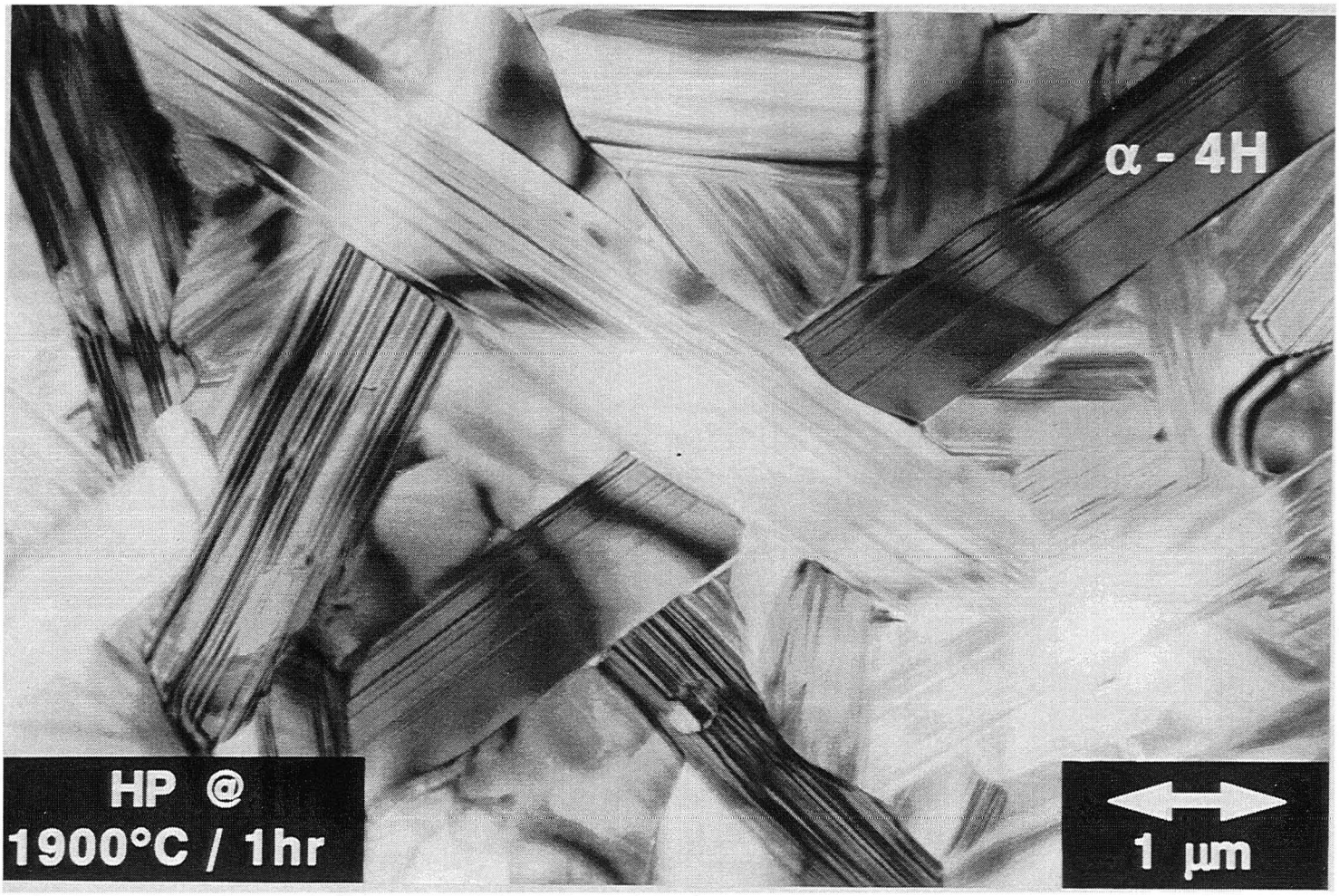

4. Bright field TEM image of the microstructure of Hexoloy-SA. Voids and regions of graphite were commonly observed in this material. The arrows indicated the predominance of ~120° triple points between equiaxed α-6H grains.

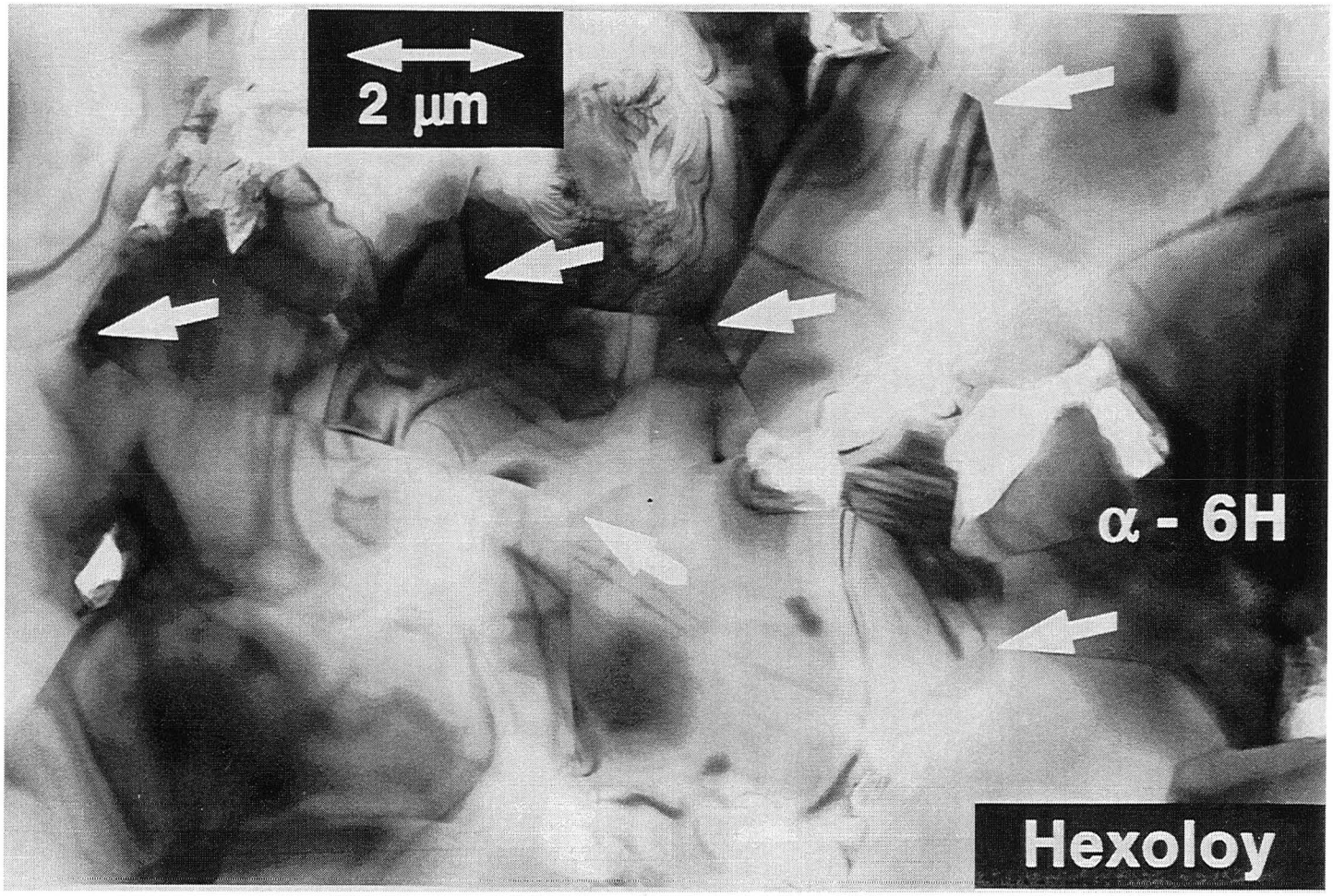

5. Bright field TEM image of a crack path along grain boundaries in ABC-SiC hot pressed at 1950°C for 1 hour. This crack was propagated by bending a doubly-dimpled TEM specimen prior to final ion beam thinning.

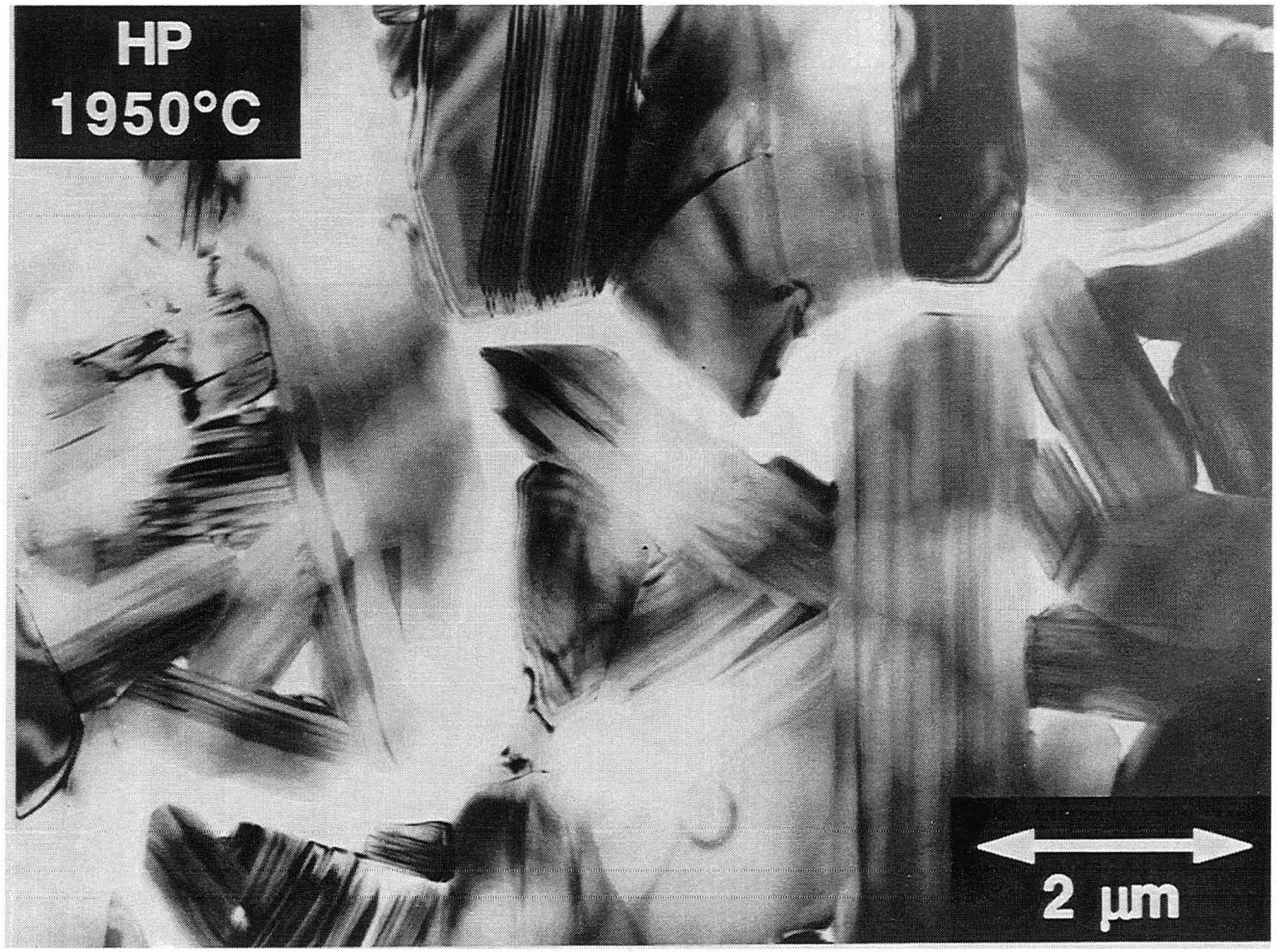

Fig. 6a.
HR-TEM image of amorphous grain boundary between an α-4H grain (<5° from a <$\bar{2}$110> orientation) and a β grain (<3° from a <110> orientation) in ABC-SiC hot pressed at 1780°C for 1 hour. The amorphous phase in ABC-SiC was typically <1 nm thick.

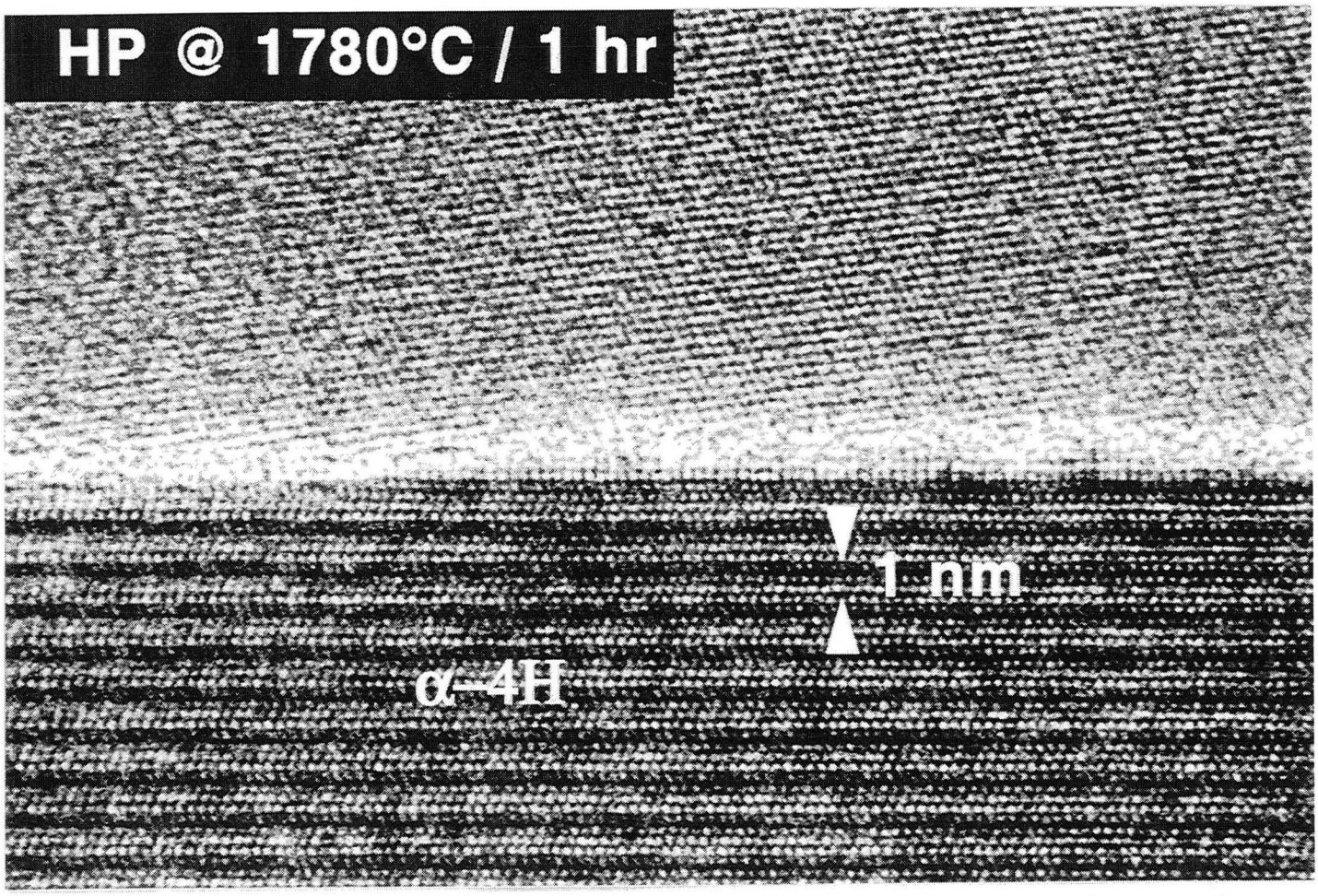

Fig. 6b.

HR-TEM image of amorphous grain boundary between two α-6H grain in Hexoloy-SA (upper and lower grains within 5° of a $<\bar{8}\ 10\ \bar{2}\ \bar{3}>$ and a $<\bar{2}110>$ orientation, respectively). Although some thick amorphous grain boundaries existed in Hexoloy-SA, the amorphous phase was typically <2 nm thick.

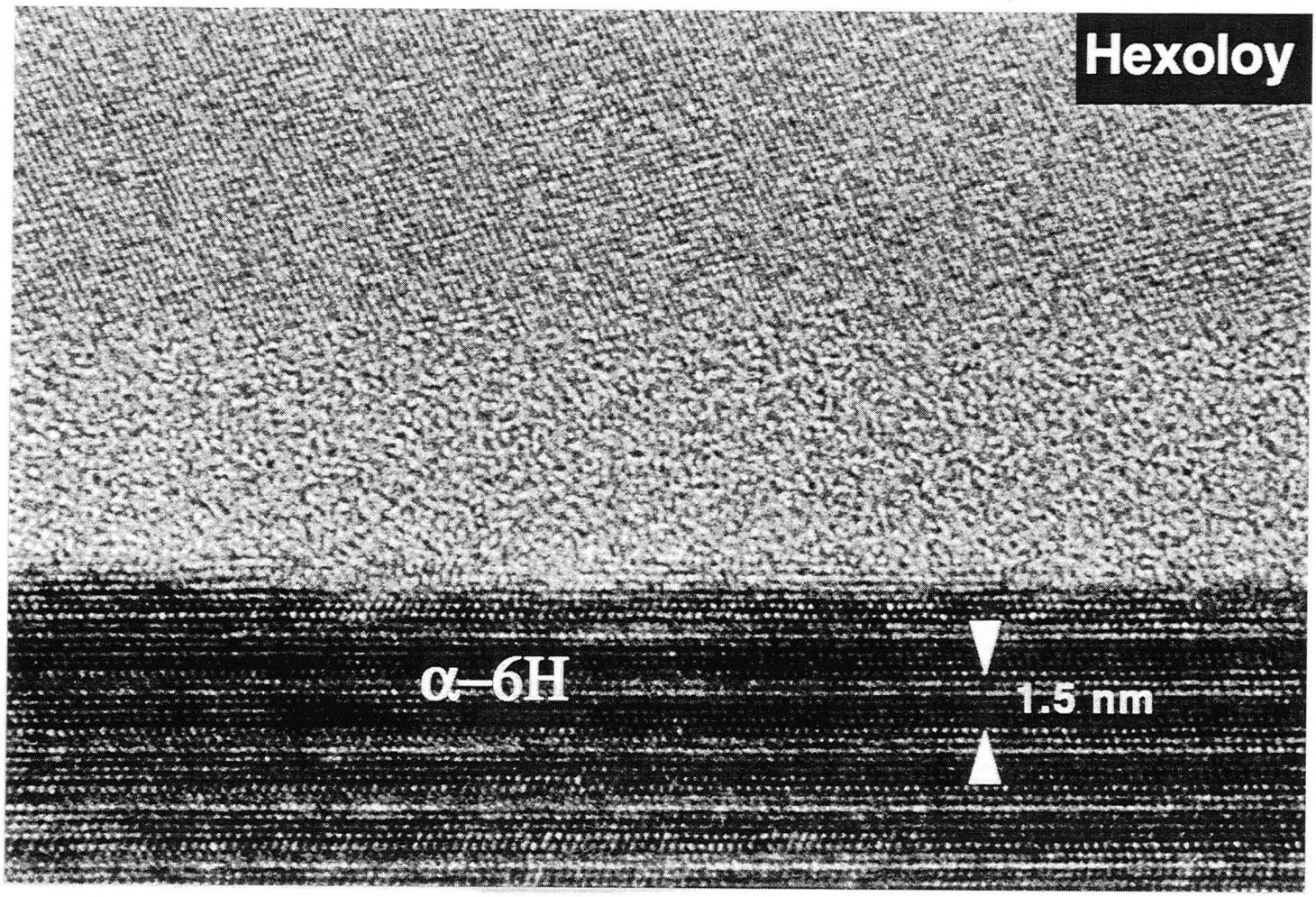

7. AES spectra acquired of an intergranular fracture surface of plate-like α-4H grains (see Figure 2a). The Al-containing amorphous phase (7a) was removed with ~1 nm Ar ion etching (7b), and only the SiC grain was detected after 2 nm etching in all grains.

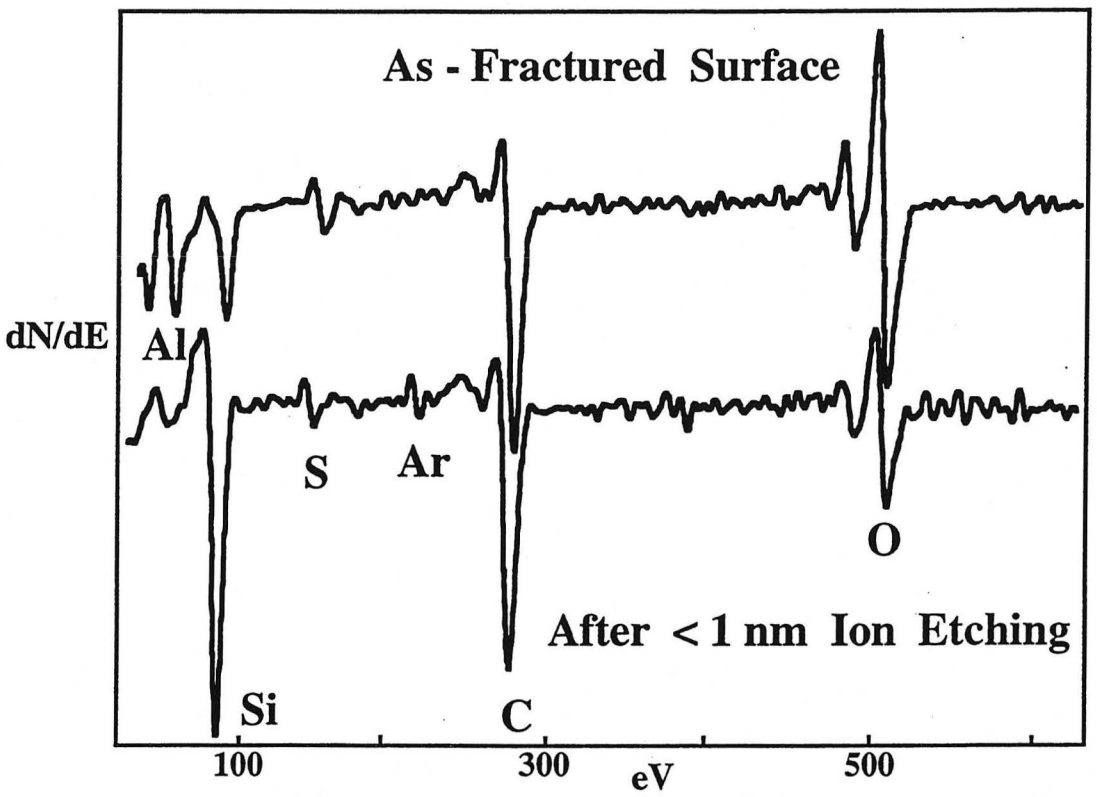

Ernest Orlando Lawrence Berkeley National Laboratory
One Cyclotron Road | Berkeley, California 94720

Prepared for the U.S. Department of Energy under Contract No. DE-AC03-76SF00098